Sedimentary geochemistry in P-limited freshwater drained marshes (Charente-Maritime, France): Original drivers for phosphorus mobilization

Raphaël Moncelon, Christine Dupuy, Philippe Pineau, Claire Emery, Eric Bénéteau, Olivier Philippine, François-Xavier Robin, Édouard Metzger

Sedimentary geochemistry in P-limited freshwater drained marshes (Charente-Maritime, France): Original drivers for phosphorus mobilization

Raphaël Moncelon [a,*], Christine Dupuy [a], Philippe Pineau [a], Claire Emery [a], Eric Bénéteau [b], Olivier Philippine [c], François-Xavier Robin [c], Edouard Metzger [b]

[a] Laboratoire LIENSs, UMR 7266, La Rochelle Université, Bâtiment ILE, 2 Rue Olympe de Gouges, La Rochelle, France
[b] Laboratoire de Planétologie et Géosciences UMR 6112, CNRS, Université d'Angers, Nantes Université, Le Mans Université, Angers, France
[c] UNIMA, 28 rue Jacques de Vaucanson, ZI de Périgny, 17180, Périgny, France

ARTICLE INFO

Editorial handling by Yi Yang

Keywords:
Drained marshes
Nutrient mobilization
Iron
Nitrate
Sulphur

ABSTRACT

Phosphorus bioavailability is a major issue in aquatic environments, where it generally limits primary production. In this work, the analysis of the pore water and the solid phase of the sediment was carried out over a 9-month monitoring period between February 2020 and April 2021 in two drained marshes (Marans and Genouillé, France) distinct by their uses and management tools. Soluble reactive phosphorus (SRP) enrichment in the sediment was intimately controlled by iron oxide dissolution. The latter seemed highly controlled by seasonal nitrate inputs (winter and early spring) that favoured denitrification as a major benthic mineralization process promoting iron curtain development and stability. Following benthic mitigation of nitrate other anaerobic metabolisms developed such as iron dissolutive reduction promoting P recycling and planktic bioavailability. Surprisingly, sulphur cycle seemed to affect P dynamics, especially in the absence of nitrate. The absence of NO_3^- triggered high sulphate reduction rates in the two first centimeters depth, reaching $-8.9\ E^{-03} \pm 0.5\ E^{-03}$ and $-5.0\ E^{-03} \pm 0.2\ E^{-03}$ nmol $cm^{-3}\ s^{-1}$ in August and July at Marans and Genouillé respectively. These values placed this process at higher rates than the denitrification (maximum in May at Marans with $-5.0\ E^{-03} \pm 1.1\ E^{-03}$ nmol $cm^{-3}\ s^{-1}$) and reduced iron production (maximum in July at Genouillé with $0.5\ E^{-03} \pm 0.1\ E^{-03}$ nmol $cm^{-3}\ s^{-1}$). The rapidity with which process changes occur (monthly scale) testified to the dynamism of these systems. The similarity in geochemical patterns regarding NO_3^- pressure at both sites underlines the importance of diffuse pollution in coastal systems for nitrogen mitigation and phosphorus trapping. The results obtained in this study could lead to the development of a generalized diagenetic operating model for temperate systems with high agricultural pressure. This would enable to target management efforts to both optimize the purification function and limit eutrophication risks in these systems.

1. Introduction

The inter-linked nitrogen (N) and phosphorus (P) cycles have been identified as one of nine important biophysical systems for the planet (Rockström et al., 2009b). If humanity should strive to adapt in these cycles, agriculture is one of the main worldwide sectors contributing to their alteration through sediment and nutrient pollution of freshwaters, particularly in the form of diffuse pollution (Wood et al., 2005; Ulén et al., 2007). This pollution results in the reduction of surface water quality affecting its ecological status, by altering growth limiting nutrient fluxes from the landscape to receiving waters (Smith, 2003; Conley et al., 2009; Sinha et al., 2017; Le Moal et al., 2019) and inducing salinization of freshwater systems (Hogan et al., 2007; Cañedo-Argüelles et al., 2013; Herbert et al., 2015). This alteration would counteract the achievement of the Water Framework Directive objectives of many European surface waters (Howarth, 2011).

Among the many ecosystem services that wetlands provide, constructed adjacent to field marshes are, in temperate environments worldwide, options available to farmers for reducing induced pollution through limiting the sediment and nutrients loss from the landscape (Vymazal, 2011; Ockenden et al., 2014 and references therein). Therefore, approaches controlling external point and non-point sources for N and P exist but are not always successful. This is partly due to the continuous release of nutrients from the sediment, that can be a real

issue (Marsden, 1989; Köhler et al., 2005; Nürnberg et al., 2012) especially in shallow waters and low hydrodynamic systems where the specific sediment surface/water volume ratio is high. This can be particularly risky in P nutrient limiting systems, frequently observed in freshwater environments (Schindler, 1977; Schindler et al., 2016; Søndergaard et al., 2017; Moncelon et al., 2021), where its release from the sediment can contribute significantly to the P demand of water column in rivers (van Dael et al., 2020), lakes (Ni et al., 2019) and even marshes (Moncelon et al., 2021). In the latter, stakes are all the highest as these systems can be connected to coastal waters, potentially sensitive to nutrient inputs and eutrophication risks. It is therefore of utmost importance to understand factors controlling P mobilization in the sediment, especially since the reduction of its external sources in agriculture can increase the effects of internal ones (Perkins and Underwood, 2001).

The sediment pore water composition is a good indicator of biological (respiration) or chemical processes involved in nutrient release and especially for soluble reactive phosphorus (SRP) in freshwater systems (Herzsprung et al., 2010). Concerning biotic respiration, the nature of the oxidant stocks, generally considered along a vertical gradient, drives the organic matter (OM) mineralization pathways in its early stages (Froelich et al., 1979; Aller, 2004). The fate and behavior of metal oxides are of particular interest in understanding the SRP remobilization in pore water. The capacity of P to adsorb on iron (Fe) or to a lesser extent on manganese (Mn) oxides (Christensen et al., 1997), prevent (Herzsprung et al., 2010) or promote its mobility and benthic recycling (Louis et al., 2021). Moreover, inhibition of iron (Fe–OOH) and manganese (MnO_2) oxides reduction by nitrate (NO_3^-) has been largely attested (Wauer et al., 2005a; Petzoldt and Uhlmann, 2006). Its inhibition effect on P mobilization was examined in few laboratory studies (Grüneberg et al., 2014) and rarely highlighted in *in situ* freshwater marshes studies (Moncelon et al., 2021, 2022). The high anthropized watersheds of French Atlantic West coast (Charente-Maritime) leads to strong NO_3^- inputs in the hydrographic system through agricultural soil leaching. Morphology and implemented water management in drained marshes seemed to impact differently nitrate inputs and fate, and therefore phosphorus bioavailability.

However, the NO_3^- effect seemed not to entirely control the fate of P mobilization, and other element such as sulphur (S) must be considered in these systems since its strong interference with iron cycle (Johnston et al., 2014). If a low sulphate (SO_4^{2-}) demand for the OM oxidation is generally considered in freshwater (Feng et al., 2014), sulphate reduction can occur at an equivalent rate than in the marine environment due to the rapid recycling of S through oxidative regeneration (Vile et al., 2003). This process could be amplified if SO_4^{2-} pollution occurs (Lamers et al., 2002) or in clay mineral composition of sediment (Stotzky and Rem, 1966; Lin et al., 2022), both potentially present in drained marshes connected to sea.

The objective of this work is to gain insights on the temporality of SRP mobilization processes within the sediment by a seasonal sampling of sediment and its pore waters throughout an annual cycle (February 2020 to April 2021). This will complete the understanding of benthos-pelagos coupling and its dynamics previously shown through the link between SRP fluxes and primary production development in drained marshes (Moncelon et al., 2021, 2022). The originality of this work resides in the comparison of two distinct anthropized freshwater marshes of Charente-Maritime differing from their distinct watersheds belonging, their implemented water management and their adjacent agricultural practices (see materiel and methods). It is supposed the strong effect of NO_3^- for P retention in the sediment, according to different water management and NO_3^- availability. First, SRP mobilization was explored in the light of the iron and nitrogen coupling under variable nitrate pressures. Then, this work attempted to examine the sulphur cycle influence and its interaction with nitrogen and finally the role in SRP mobilization in freshwater marshes connected to sea.

2. Material and methods

2.1. Study sites

Two eutrophic freshwater marshes of Charente-Maritime being part of the large group of maritime marshes of the French oceanic coastline were chosen according to their distinct specific characteristics (Tortajada et al., 2011; Moncelon et al., 2021). Study sites are portions of secondary channels belonging to the Sèvre Niortaise (Marans site, 46.282°, 0.969°) and the Charente Maritime (Genouillé site, 45.998°, −0.794°) artificial hydrographic networks (Fig. S1, supplementary material). Their respective catchment areas are about 690 and 870 km^2 (Water Development and Management Plan of the Sèvre Niortaise and Charente (SAGE)). The two sites differ 1) by the nature of the activities that surround them, the watershed of the Marans site being dominated by cereal crops (75% of the drained marsh), while that of Genouillé is surrounded by both cattle lands and crops (surrounded by permanent grasslands) 2) by the physical structure of the canal, about 1.60 m deep for 6 m wide for Marans and 0.80 m deep for 4 m wide for Genouillé and, 3) by the management modalities of the water reserve (recharging by groundwater and rainfall in Marans, rainfall and pumping of the Charente River in Genouillé). Although no data was recorded informing about water fluctuation (water discharge through sea locks gates, flow rate, height), channels were always flooded during the sampling periods.

2.2. Sediment sampling and processing

Sediment cores were sampled manually with 10 cm-diameter and 30 cm-long PVC tubes in both sites. Field campaigns were realized two months out of three between February 2020 and April 2021 (June, September, December 2020 and February and March 2021 were not sampled). For every sampling time, three cores were sampled for each site with taking care to keep a water thickness of at least 5 cm above the sediment to preserve the sediment-water interface and for bottom water chemistry.

2.2.1. Dissolved phases

Overlying water was extracted from each core and filtered through a 0.2 µm RC25 Sartorius filter. Cores were then sliced under gaseous nitrogen every 5 mm down to 6 cm depth to avoid oxidation of solid and dissolved phases. Pore water was extracted by centrifugation (2000g during 20 min at site temperature) and filtered using a 0.2 µm RC25 Sartorius filter.

Overlying and pore water were conserved at −20 °C for nutrients analyses (see below), and an aliquot was conserved at 5 °C for silica analysis. Other aliquots were immediately used for alkalinity measurement and HNO_3 acidified (0.01 mol L^{-1}; Suprapur Merck) for metal analysis. Nutrients *i.e.* nitrate (NO_3^-), nitrites (NO_2^-), soluble reactive phosphorus (SRP), ammonium ($\sum NH_3$) and silica (Si) concentrations were determined by a colorimetric autoanalyser Scalar Seal (detection limit of 0.02 µmol L^{-1}). The acidified aliquots were analyzed by ICP-AES (Thermo Scientific iCAP 6300 Radial) to measure dissolved iron (total iron, mentioned as Fe_d), manganese (Mn^{2+}, mentioned as Mn_d), sulphur (S_d), and sodium (Na_d) after a 10-times dilution using a 10^{-2} mol L^{-1} HNO_3 suprapur solution (detection limit about 1 µmol L^{-1} considering dilution). Total dissolved sulphur (S_d) is interpreted as sulphate (SO_4^{2-}) concentration as samples were acidified favouring sulphide degassing (Metzger et al., 2007). Alkalinity (alk) was determined according to the colorimetric method from Sarazin et al. (1999). Absorbance measurements were carried out with a spectrophotometer (SPECTROstar Nano, BMG LABTECH) at 590 nm.

Production and consumption rates of dissolved species (NO_3^-, Mn_d, Fe_d, S_d and SRP) were determined using the Profile software integrated on the entire sediment column sampled (Berg et al., 1998).

2.2.2. Solid phases

Remaining sediment was freeze-dried, grounded and conserved at ambient temperature and dry environment in the dark for solid phase analysis. An aliquot (~100 mg) was used for the ascorbate extraction of reactive manganese (Mn^{3+} and Mn^{4+}, mentioned as Mn_{asc}), iron (amorphous Fe^{3+}, mentioned as Fe_{asc}) and P according to the method used in Kostka and Luther (1994) and Anschutz et al. (1998). Samples were analyzed by ICP-AES. Errors on final concentrations are about 10–15 %.

An aliquot (~15 g) was used for Organic Matter (OM) quantification by combustion loss at 430 °C (Davies, 1974). Data are expressed in percentage of dry weight (dw %).

2.3. Statistical tests

Correlation tests were applied on pore water parameters and made with the software R studio (February 1, 1335). Kendall rank-based correlation test was used according to the non-normality of residues. Correlations were therefore presented through Kendall correlation coefficient τ.

3. Results

3.1. Organic matter content

OM content in the solid fraction fluctuated between 9 and 17 % during the survey period at both sites (Fig. 1), without showing marked vertical gradients excepted for some local enrichments up to 19 % observed during summer (Marans, July 2020, Fig. 1 A). OM may have increased from 10 to 17% between February to August 2020 at Marans and remained between 14 and 15 for the rest of the survey (Fig. 1 A). At Genouillé, OM varied from 9 % (February–May 2020) to 16 % (July–October 2020) then decreased to 14 % (November 2020–April 2021) with a slight enrichment in surface (Fig. 1 B).

3.2. Redox sensitive elements in the sediment

The global decrease of NO_3^- and NO_2^- concentration in the superficial water from February to October 2020, seemed to result in the decrease of their pore water concentration and in the decrease of their penetration depth (Fig. 2). At Marans, NO_3^- and NO_2^- penetrated the sediment from February to May 2020 and from November to April 2021 up to 1 cm depth (Fig. 2 A). Maximum NO_3^- (500 µmol L^{-1}) and NO_2^- (35 µmol L^{-1}) were observed in January 2021 (Fig. 2 A 50) and November 2020 (Fig. 2 A 43) respectively. At Genouillé, it penetrated the first centimeters of sediment in May (maximum at 200 and 2 µmol L^{-1} for NO_3^- and NO_2^- respectively, Fig. 2 B 15), in January 2021 for NO_3^- (maximum at 200 µmol L^{-1}, Fig. 2 B 50) and from November 2020 to January 2021 for NO_2^- (maximum at 12 µmol L^{-1}, Fig. 2 B 43,50).

Sediment surface Mn_d concentration increased from July to October 2020 and then in April 2021 at Marans, coinciding with shallower NO_3^- penetration in the sediment, with maximum concentration at 50 µmol L^{-1} at 1 cm depth in October 2020 (Fig. 2 A 37) and April 2021 (Fig. 2 A 58). At Genouillé, it increased between 0 and 6 cm depth all along the survey with sharpest gradients in the 2 first centimeters (maximum concentration at 6 cm depth at 100 µmol L^{-1} in October, Fig. 2 B 37). The first centimeter was partly depleted especially from February to May 2020 (Fig. 2 B 2, 9, 16 respectively) and in January 2021 (Fig. 2 B 51) (below 20 µmol L^{-1}), coincided with NO_3^- penetration in the first centimeter depth. Mn_{asc} fluctuated between 2 and 4 mmol kg^{-1} at both Marans and Genouillé. Conversely to Mn_d, Mn_{asc} seemed to present significative redox fronts with higher concentrations within the 2 first centimeters depth, especially from February to May 2020 (Fig. 2 A 2,9,16), and from November 2020 to January 2021 (Fig. 2 A 44, 51) at Marans coinciding with NO_3^- and/or NO_2^- penetration in the sediment (Fig. 2 B 2, 16, 44, 51 at Genouillé).

Fe_d was positively correlated with Mn_d in pore water (Table 1). At Marans, τ is comprised between 0.327 (July 2020, $p < 0.01$) and 0.896 (February 2020, $p < 0.001$). At Genouillé, higher τ were calculated, from 0.571 (May 2020, $p < 0.001$) to 0.910 (February 2020, $p < 0.001$). A first Fe_d pore water enrichment occurred between 2.5 and 5 cm depth from February to May 2020 (peak at 120 µmol L^{-1}) at Marans (Fig. 2 A 3, 10, 17). Then Fe_d followed the same patterns as Mn_d. Mobilization zone reached the sediment water interface (SWI) from July to November 2020 (maximum between 1 and 3.5 cm depth, >60 µmol L^{-1}, Fig. 2 A 24, 31, 38, 45). At Genouillé, Fe_d mobilization intensified from 1.5 cm depth to core bottom from February to May 2021 (Fig. 2 B 3, 10, 17) and was closer to the SWI from July to November 2020 (Fig. 2 B 24, 31, 38, 45). Pore water enrichment was the highest at that site between 4 and 6 cm depth from October to November, to reach ~400 µmol L^{-1}. From November 2020 to April 2021 the first 1.5 cm were nearly depleted of Fe_d (Fig. 2 B 45, 52, 59). Unlike dissolved manganese, dissolved iron was never detected in the overlying water. At Marans, Fe_{asc} fluctuated between 30 and 65 mmol kg^{-1} from February to July 2020 and from January to April 2021. It was <30 mmol kg^{-1} from August to November 2020 (Fig. 2 A 31, 38, 45). At Genouillé, Fe_{asc} fluctuated between 25 and 50 mmol kg^{-1} with higher concentrations on the first centimeter depth in November 2020 and January 2021 (Fig. 2 B 45, 52), coincided with NO_3^- and/or NO_2^- penetration.

SRP increased in the pore water between 4 and 6 cm depth from February to May 2020 at Marans, with maximum concentration about 30 µmol L^{-1} in April (Fig. 2 A 4, 11, 18). From July to November 2020, it mobilized in a larger part of the sedimentary column to reach the SWI (Fig. 2 A 25, 32, 39, 46). Enrichment was at its highest at 6 cm depth in August (35 µmol L^{-1}). P_{asc} fluctuated between 4 and 10 mmol kg^{-1} with globally higher concentration from April to August 2020 (Fig. 2 A 11, 18, 25, 32) and from January to April 2021 (Fig. 2 A 53, 60). At Genouillé, SRP increased from February to August 2020 from 2

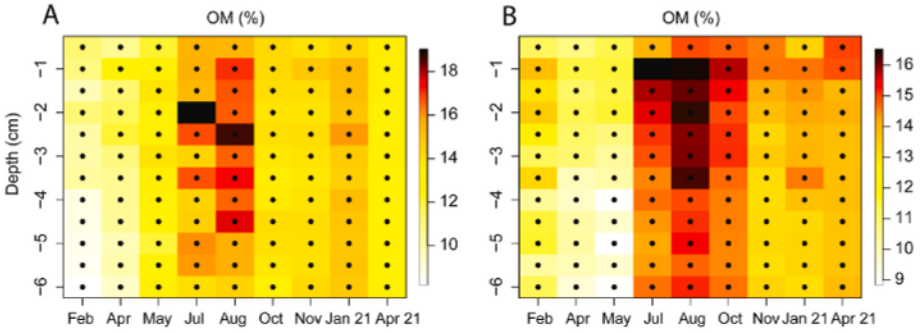

Fig. 1. Organic matter content (OM, %) in sediment from 0 to 6 cm depth at Marans (A) and Genouillé (B), from February 2020 to April 2021. Black points represents the sampling steps.

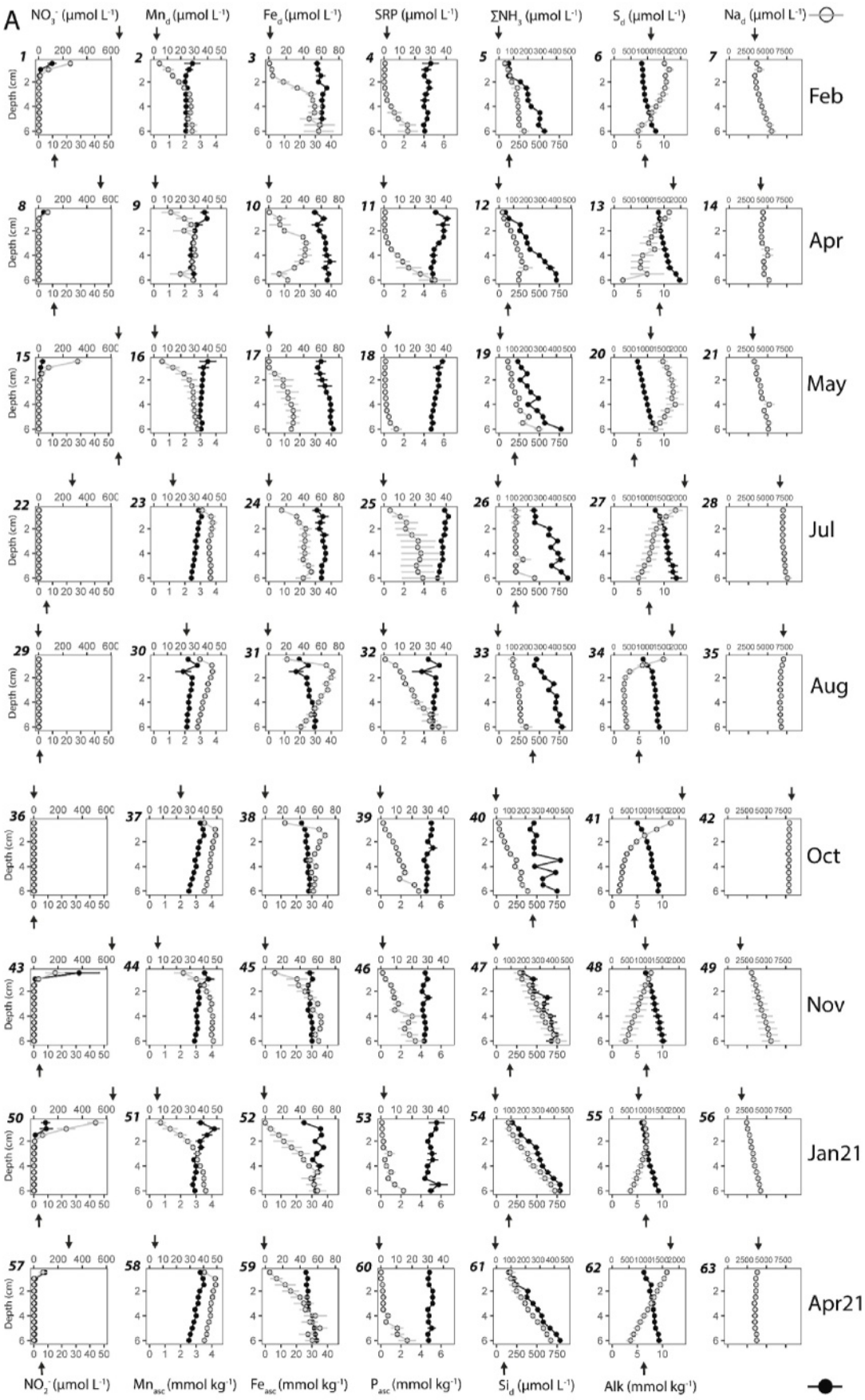

Fig. 2. Nitrogen (NO_3^-, NO_2^-, ΣNH_3), phosphorus (SRP, P_{asc}), Si, iron (Fe_d, Fe_{asc}), manganese (Mn_d, Mn_{asc}), sulphur (S_d, S_{asc}) and alkalinity (alk) profiles in sediment from 0 to 6 cm depth at Marans (A) and Genouillé (B), from February 2020 to April 2021. Black arrows represent overlying water concentrations.

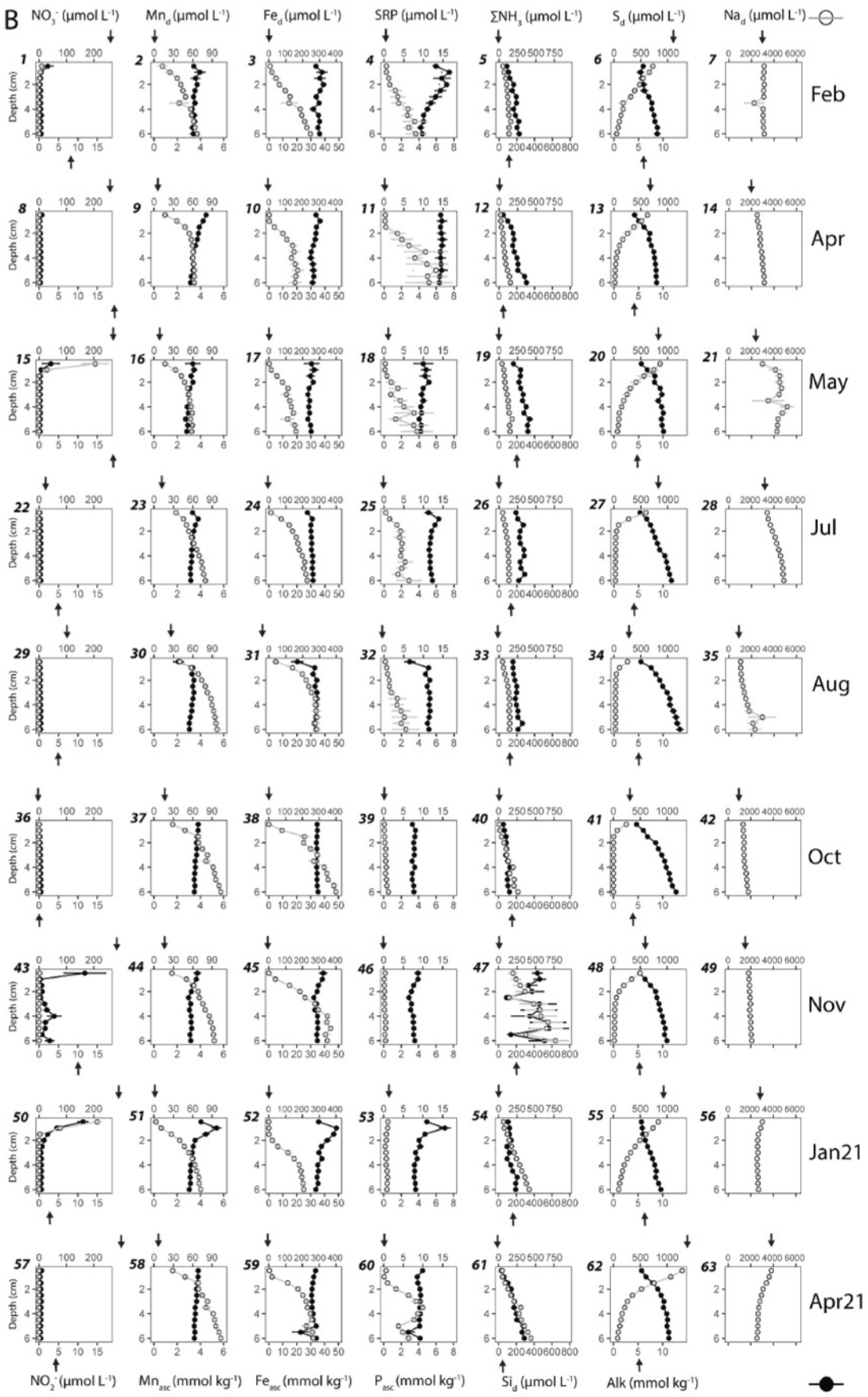

Fig. 2. (*continued*).

Table 1
Correlation (Kendall coefficient τ) between dissolved iron (Fe_d), manganese (Mn_d), sulphure (Sd) and phosphorus (SRP) at Marans and Genouillé, from February 2020 to April 2021. *** p < 0.001; ** p < 0.01; * p < 0.05.

		Mn_d vs Fe_d		Fe_d vs SRP		S_d vs SRP	
	date	t	*p*	t	*p*	t	*p*
Marans	Feb	0.896	***	0.4	***	−0.464	***
	Apr	0.503	***	0.184		−0.473	***
	May	0.793	***	0.448	***	−0.396	***
	Jul	0.327	**	0.171		−0.73	***
	Aug	0.67	***	−0.171		−0.394	***
	Oct	0.6	***	−0.073		−0.635	***
	Nov	0.583	***	0.609	***	−0.723	***
	Jan21	0.822	***	0.499	***	−0.701	***
	Apr21	0.476	***	0.662	***	−0.736	***
Genouillé	Feb	0.91	***	0.896	***	−0.661	***
	Apr	0.737	***	0.503	***	−0.603	***
	May	0.571	***	0.793	***	−0.589	***
	Jul	0.806	***	0.327	**	−0.117	
	Aug	0.81	***	0.67	***	−0.514	***
	Oct	0.689	***	0.6	***	−0.287	*
	Nov	0.892	***	0.583	***	−0.125	
	Jan21	0.876	***	0.822	***	−0.206	
	Apr21	0.679	***	0.476	***	−0.37	**

(February–May), 1.5 (July) and 3 (August) cm depth to core bottom (Fig. 2 B 4, 11, 18, 25, 32). Enrichment was at its peak in April, between 3.5 and 6 cm depth. Almost total SRP depletion was observed from October 2020 to January 2021 (Fig. 2 B 39, 46, 53), before re-increase in April 2021 between 2 cm and the core bottom. Enrichment period of P_{asc} in the sediment coincided with that of SRP. It fluctuated between 4 and 7 mmol kg^{-1} from February to August 2020 and from January (2.5 first centimeters) to April 2021. It depleted at nearly 3 mmol kg^{-1} from October to November 2020 on the entire core thickness.

In the overlying waters and the top core (0–2 cm depth) of Marans site, S_d fluctuated between 1200 and 1800 µmol L^{-1} from February to July, with slight decrease from SWI to 2 cm depth (Fig. 2 A 6, 13, 20,27). S_d was strongly depleted between 2 and 6 cm depth (~300 µmol L^{-1}) from August to October (Fig. 2 A 34, 41), before re-increase above 800 µmol L^{-1} from November to April 2021. It was negatively correlated with SRP for each month ($p < 0.001$, Table 1). At Genouillé, S_d was >100 µmol L^{-1} between SWI and 4 cm depth from February to May 2020 (Fig. 2 B 6, 13, 20). From July to November 2020, strong S_d depletion occurred (around 20 µmol L^{-1}) between 1.5 and 6 cm depth (Fig. 2 B 27, 34, 41, 48). It re-increased from January to April 2021 to reach around 1000 µmol L^{-1} at the SWI.

Alkalinity increased with depth at both sites, fluctuating between 5 and 13 mmol L^{-1}. It reached highest values in April and July 2020 at Marans (Fig. 2 A 13, 27), and from July to October 2020 at Genouillé (Fig. 2 B 27, 34, 41).

$\sum NH_3$ profiles showed similar patterns at both sites. It presented positive gradient of concentration with depth, with highest concentration observedfrom November to April 2021 at 6 cm depth (Fig. 2 A/B 47, 54, 61). Maximum concentrations were about 400 and 750 µmol L^{-1} in November at Marans and Genouillé respectively.

Dissolved silica (Si_d) fluctuation globally followed that of $\sum NH_3$. It showed an increase with depth and highest concentrations in the entire core from July to October (between 500 µmol L^{-1} at the top of the core and 800 µmol L^{-1} in depth at Marans (Fig. 2 A 26, 33, 40). At Genouillé, Si_d maximal concentrations were observed in November around 750 µmol L^{-1} at 6 cm depth (Fig. 2 B 47).

3.3. Sodium in pore water

Dissolved sodium showed little vertical variability during the survey period at Marans. From February to May 2020, it remained roughly stable about 4 mmol L^{-1} (Fig. 2 A 7, 14, 21) then increased to reach 8 mmol L^{-1} in October (Fig. 2 A 42) and rapidly decreased to the winter values previously measured. At Genouillé, Na_d also showed a seasonal trend with lowest values in winter, late summer and fall (down to 2.5 mmol L^{-1}). Highest concentrations were observed between May and July 2020 (between 4 and 5 mmol L^{-1}) (Fig. 2 B 21, 28).

4. Discussion

4.1. Monthly temporality of P remobilization

4.1.1. Organic origin of SRP

The positive correlation between SRP and Fe_d at Genouillé in October and November 2020 (Table 1, $\tau > 0.580$, $p < 0.001$) followed a 1/424 SRP/Fe_d ratio, especially in November (Fig. 3 B). This ratio corresponds to a SRP enrichment through OM mineralization through iron oxide reduction according to stoichiometry of Froelich et al. (1979). This strongly supports the idea of an organic origin phosphorus enrichment in porewater at that time. However, this organic P enrichment was minor compared to other periods and, therefore, is not sufficient to explain the SRP increase at other months. This was significantly highlighted in April 2021 at Marans (Fig. 3 A) and in May 2020 at Genouillé (Fig. 3 C), where SRP enrichment was closer to a 1/2 SRP/Fe_d ratio, highlighting a mobilization by dissolution of iron oxides (Gächter and Müller, 2003).

Mn_d enrichment showed congruent pattern with those of Fe_d, which may suggest concomitant Mn and Fe oxide respiration for OM mineralization (Fig. 2, Table 1). However, the SRP/Mn_d ratio far above that of Froelich (SRP/Mn_d = 1/236) in most of pore water sampled at both sites (Fig. 4C and D) suggest another contribution than organic matter. Moreover, the SRP enrichment zones far below that of NO_3^- and S_d consumption zones also discard a contribution of denitrification and sulphate reduction to P benthic mobilization.

4.1.2. Mineral origin of SRP

If N is supplied almost entirely in the form of organic nitrogen, detrital phosphate minerals (e.g. apatite) and phosphate adsorbed on hydrolyzates and oxidates (e.g. clays and ferric hydroxide) probably contribute to phosphorus bulk. The non-coincidence between the SRP and $\sum NH_3$ profiles (the latter often used as a witness to anaerobic OM mineralization) supports the fact that the SRP can come from the dissolution of mineral phases. This was also suggested since no correlation with SRP and $\sum NH_3$ fluxes were observed in intertidal mudflat works (Louis et al., 2021). This lack of correlation was also observed in freshwater Charente Maritime marshes (Moncelon et al., 2022).

Most of the sediment column indicated potential precipitation of metastable Fe^{3+}-compounds containing phosphate (SRP/Fe_d < 0.5) (Gächter and Müller, 2003). On the first centimeter, these ratios may have been higher outside summer period due to the rapid Fe_d oxidation (Fig. 4A–C). Moreover, P_{asc}/Fe_{asc} fluctuated between 0.10 and 0.25 throughout the sampling period at both sites (Fig. 5A and B). The P_{asc}/Fe_{asc} ratios always <0.5 testified the unsaturation of iron oxide binding sites. This highlighted a rapid sorption of mobilized P onto iron hydroxides and a constant trapping capacity for phosphorus. These ratios are in the same orders of magnitude as those calculated in various salty coastal environments (Thibault de Chanvalon et al., 2017 and reference therein). In this study, the strongest ratios were observed from July to October 2020 and from April to August 2020 at Marans and Genouillé respectively. Lower ratios were reached in winter and spring at Marans and from October 2020 to April 2021 at Genouillé. These changing trends could have an impact on the residence time of SRP in the sediment.

The depth of precipitation threshold between SRP and Mn_d (SRP/Mn_d = 0.2, Christensen et al. (1997)) fluctuated between 3.5 and 5.5 cm in winter and spring and went up between 1 and 2.5 cm depth in summer and fall at Marans (Fig. 4 C). At Genouillé, SRP/Mn_d was globally always

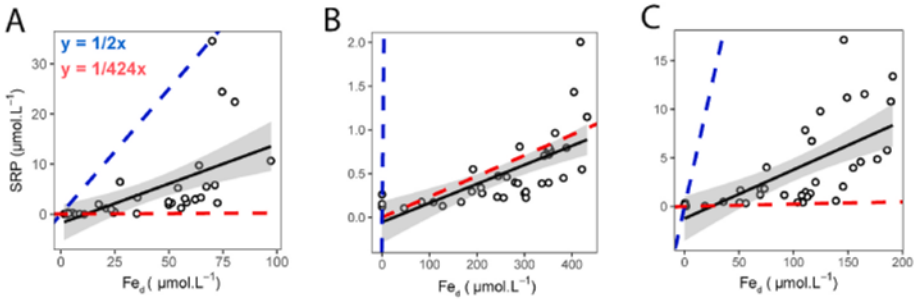

Fig. 3. Example of relationship between dissolved iron (Fe_d) and SRP in April 2021 at Marans (A) and in October and May 2020 at Genouillé (B and C respectively). Blue dashed line represent the mineral mobilization of SRP according to desorption on iron oxides (based on the minimum molar stoichiometric 1(P)/2(Fe) ratio of the solid FeOOH–P, Gächter and Müller, 2003). Red dashed line represent the organic mobilization of SRP by iron oxide reduction according to the 1(SRP)/424(Fe_d) ratio of Froelich et al. (1979).

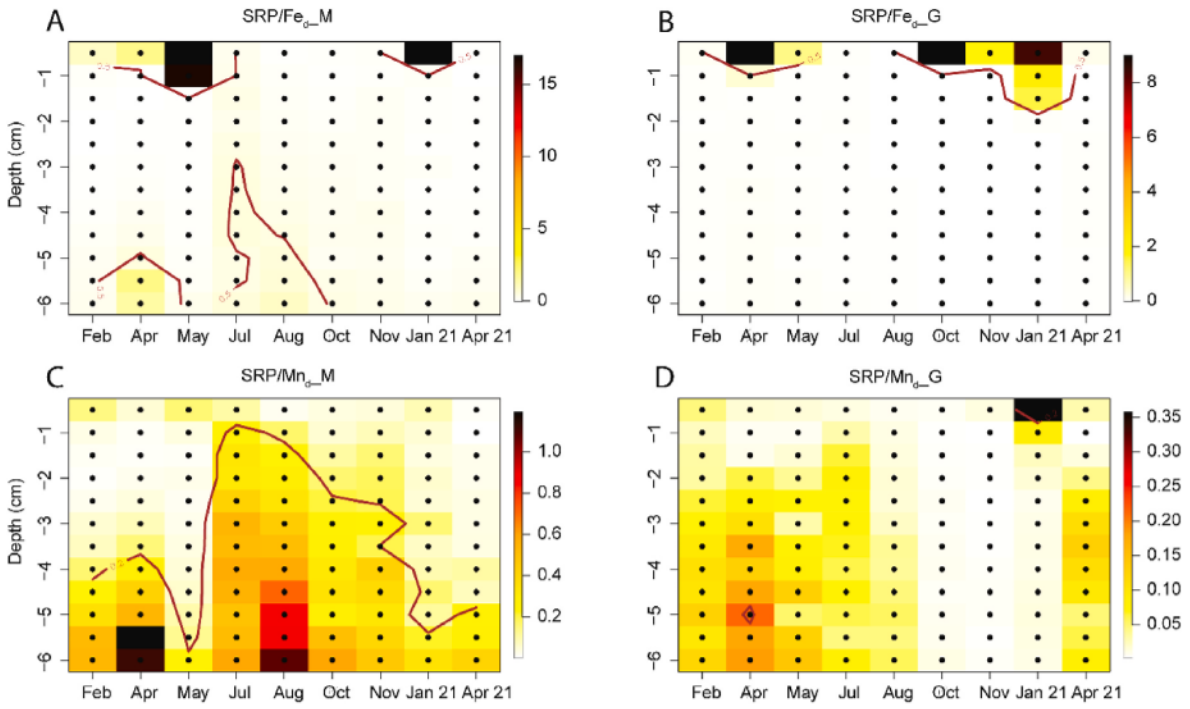

Fig. 4. SRP/Fe_d and SRP/Mn_d in sediment from 0 to 6 cm depth at Marans (A and C respectively) and Genouillé (B and D respectively), from February 2020 to April 2021. Black points represents the sampling steps. Brown lines represents precipitation ratio of iron and manganese according to Gächter and Müller (2003) and Christensen et al. (1997) respectively.

<0.2 (lowest ratios between October 2020 and January 2021, Fig. 4 D), as observed in April 2020 from 3.5 cm depth. Even though SRP/Mn_d ratios of both sites indicated the potential precipitation of metastable Mn^{4+}-compounds containing phosphate, the permanent P_{asc}/Mn_{asc} > 0.2 all along the sampling period (Fig. 5C and D) testify the saturation of Mn oxide binding sites (Christensen et al., 1997) and a weaker sequestration role of Mn for P.

Here, positive correlation between pore water SRP and Fe_d at both sites (observed in August and October 2020 at Marans, Table 1) could suppose an inorganic P origin through iron oxide respiration. This was supported by the clear excess of SRP mobilization observed over the organic mobilization created by iron oxide respiration most of the time (October and November 2020 at Genouillé, Fig. 3). These correlations were stronger at Genouillé and more constant over the survey, between 0.327 ($p < 0.01$) in July 2020 and 0.896 ($p < 0.001$) in February 2020 (Table 1). This could indicate a more direct link between Fe and P mobilization on this site.

Other processes at work releasing SRP, within or even deeper the studied sediment column, were however suggested. The latter was supported by both the non-matching Fe_d and SRP enrichment zones in pore water and the Fe_d mobilization above that of SRP (e. g. April at Marans, Fig. 2 A 10, 11). This mismatch could be explained by different precipitation kinetics of Fe and P species and the much faster precipitation of Fe_d (Millero et al., 1987) than that of P (Neupane et al., 2014). Moreover, the no significantly lower surface P_{asc} concentrations (than that of the bottom of the cores) invalidates the hypothesis of a less rich P deposited sediment nature during the more recent sedimentation phases which might have caused such vertical mismatch.

The mineral contribution in SRP from Mn oxide dissolution in the sediment column studied was unlikely to explain the surplus of SRP observed according to iron oxide respiration. This was supported by the lower SRP release potential of Mn oxide dissolution far lower from that of Fe and the staggered Mn_d and SRP enrichment zones.

4.2. *Seasonal temporality of SRP efflux under NO_3^- influence*

Despite potential constant trapping capacity (through iron oxides) and monthly variability in SRP enrichment period, SRP diffusive effluxes

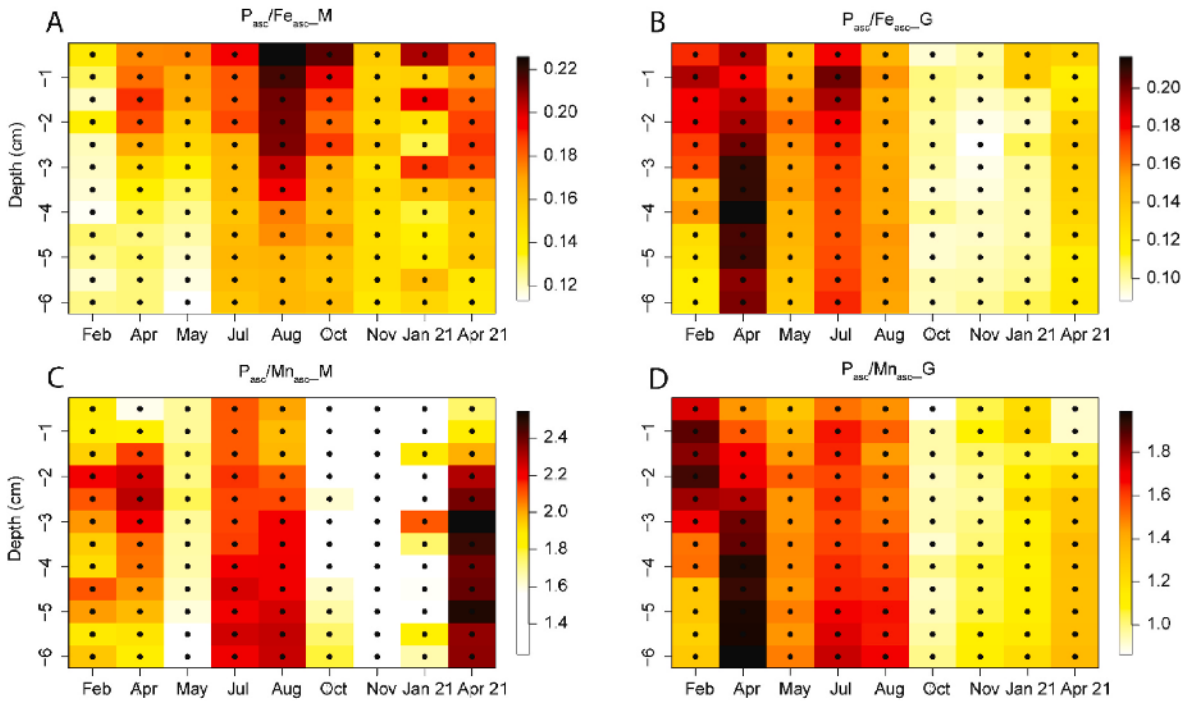

Fig. 5. P_{asc}/Fe_{asc} and P_{asc}/Mn_{asc} in sediment from 0 to 6 cm depth at Marans (A and C respectively) and Genouillé (B and D respectively), from February 2020 to April 2021. Black points represents the sampling steps.

have been calculated at a seasonal scale. They presented significant seasonal variability inversely correlated with nitrates influxes (Moncelon et al., 2022). The highest nitrate penetration rates in sediment coincided with the lowest Fe_d and SRP production. (Table 2). Conversely, in the absence of NO_3^- penetration (i. e. August and July in Table 2), Mn_d and Fe_d production increased by an average of about 57% and 325% respectively between May and August at Marans. At Genouillé, if Mn_d production decreased about 60% in July (with the absence of pore water nitrate and maximal SRP effluxes), Fe_d production increased by 663%. These shifts in iron production coincided with the apperance of SRP production in the sediment in August and July ($1.8\ E^{-05} \pm 1.3\ E^{-05}$ and $0.7\ E^{-05} \pm 0.5\ E^{-05}$ nmol cm^{-3} s^{-1} at Marans and Genouillé respectively).

Nitrate could inhibit phosphorus mobilization (and subsequent benthic efflux) by inhibiting diagenetic iron recycling. In winter and spring at both sites NO_3^- penetration and its rapid depletion in the two first centimeters depth could highlight denitrification processes at the expense of other anaerobic mineralization processes (such as metal oxide reduction or sulphate reduction) in such layer. The near total depletion of Fe_d in the surface layers of sediment when NO_3^- penetrates (February–May 2020 and November 2020–April 2021), as well as the rise of the Fe_d mobilization zone when NO_3^- was absent (between July and October 2020) at both sites seemed to confirm the inhibition of iron oxide respiration by denitrification processes. This is in accordance with the preference of denitrification for the mineralization of OM in anaerobic conditions (Froelich et al., 1979). At the concentration range recorded during this survey, NO_3^- can be the preferential electron acceptor in the bacteria and denitrifying protozoa consortium for OM mineralization, even in presence of oxygen (Chen et al., 2005; Glock et al., 2019; Zhu et al., 2020). This strong nitrate consumption (and thus the inhibition of iron oxide respiration) is in line with the observations of Moncelon et al. (2021) in winter 2019 at Marans site. However, this inhibition also seemed to occur until spring and autumn 2020, which confirmed the importance of punctual NO_3^- pulses from high anthropized basins on the sediment redox system and SRP benthic recycling (Moncelon et al., 2022).

Inhibition of both iron oxide respiration and SRP enrichment led by NO_3^- consumption did not seem to affect all the entire sampled sediment column. SRP enrichment was observed in depth despite NO_3^- penetration in the 2 first centimeters depth. Indeed, the absence of NO_3^- between July and October 2020 at Marans seemed to allow a rise of SRP near the SWI, which increased the outflow of SRP towards the water column and its bioavailability for primary production (Moncelon et al., 2021, 2022). This was observed to a lesser extent in Genouillé in July and August. The probable depletion of the mineral P stock (main source of SRP) in the sedimentary compartment at Genouillé between August 2020 and

Table 2
Production/consumption data of NO_3^-. Mn_d. Fe_d. S_d and SRP integrated on the sediment depth sampled in May and August for Marans and May and July for Genouillé. These results are based on a two-month comparison contrasted by the SRP effluxes (low or null in May. and maximum in July and August at Genouillé and Marans respectively) from Moncelon et al., (2022). and by the NO_3^-/NO_2^- penetration in the sediment (maximal in May and null in July and August). NA corresponds to the below detection limit values.

		Marans 2020								Genouillé 2020							
		May				August				May				July			
prod./cons. nmol cm^{-3} s^{-1}	NO_3^-	−5.0	±	1.1	E^{-03}	NA				−4.4	±	0.9	E^{-03}	NA			
	Mn_d	0.5	±	0.2	E^{-04}	0.9	±	0.1	E^{-04}	1.3	±	0.2	E^{-04}	0.8	±	0.2	E^{-04}
	Fe_d	0.6	±	0.5	E^{-04}	2.7	±	0.9	E^{-04}	0.6	±	1.1	E^{-04}	4.7	±	1.2	E^{-04}
	S_d	2.5	±	0.2	E^{-03}	−0.9	±	0.5	E^{-03}	−1.1	±	1.1	E^{-03}	−5.0	±	0.2	E^{-03}
	SRP	−3.0	±	1.4	E^{-05}	1.8	±	1.3	E^{-05}	−0.6	±	1.0	E^{-05}	0.7	±	0.5	E^{-05}

January 2021 could explain that such evidence was not observed at that time. This depletion could be supposed through the concomitant SRP and P_{asc} decrease at that time (Fig. 2 B 39, 46).

The presence of NO_3^- in the top sediment must be linked to reoxidation processes of reduced inorganic metabolites such as Fe and Mn (Thamdrup and Canfield, 2000; Herzsprung et al., 2010). Indeed, biological ferrous iron oxidation led by denitrifying (Hauck et al., 2001), Anaerobic Ammonium Oxidation (Anammox) (Oshiki et al., 2013) or phototrophic Fe(II)-oxidizers (Melton et al., 2012) bacteria could explain the Fe_d depletion when NO_3^- pulses occurred. The increase of metal oxides content (Fe_{asc}, Mn_{asc}) in topmost layer of the sediment at both sites when NO_3^-/NO_2^- pulses occurred, suggested such re-oxidation processes (e. g. from February to May 2020 at Marans, Fig. 2 A 2, 9, 16, and in January 2021 at Genouillé, Fig. 2 B 52). This could contribute to the efficiency of the P bound Fe (Fe–P) curtain at the SWI, by improving the capacity of iron oxides to adsorb phosphates, and thus prevent P transfer toward the water column (Christensen et al., 1997; Herzsprung et al., 2010).

4.3. Sulphur, an unexpected player

4.3.1. Sulphate reduction and associated SRP mobilization

Since its strong interference with Fe (and thus P) cycle, S dynamics must be considered in these environments (Johnston et al., 2014). Strong S_d depletion between August and October 2020 at Marans (Fig. 2 A 34, 41) and between July and November at Genouillé (Fig. 2 B 27, 34, 41, 48) suggested higher sulphate reduction rates between 0-3.5 and 0–1 cm depth at Marans and Genouillé respectively compared to other months. Consumption of $-0.9\ E^{-03} \pm 0.5\ E^{-03}$ nmol $cm^{-3}\ s^{-1}$ and $-5.0\ E^{-03} \pm 0.2\ E^{-03}$ nnmol $cm^{-3}\ s^{-1}$ were observed in August and July at Marans and Genouillé respectively (Table 2).

The depth where sulphate reduction occurred was always below the nitrate penetration depth, leading to consider the inhibition of denitrification on sulphate reduction. Such inhibition rate have been recorded up to 82% in strong presence of denitrifying bacteria (7.6×10^4 CFU·(100 mL)$^{-1}$, Jin et al., 2017). The absence of NO_3^- penetration coincided with appearance of S_d consumption (August, Marans) or its increase (about 350% in July, Genouillé) (Table 2).

The highest P effluxes were concomitant with the highest Fe_d production and S_d consumption rates, in August (Marans) and July (Genouillé) 2020 (Table 2). More than explain the potential co-occurrence of iron and sulphate reduction at that time (Bethke et al., 2011; Ma et al., 2017), this coincidence could be used to explain interaction between Fe and S promoting the SRP efflux. When S_d consumption was maximum in the 2 first centimeters depth particularly in August and October 2020 at Marans, the highest Fe_d mobilization was too. This suggested that sulphide produced by sulphate reduction could reduce iron oxides and therefore increase pore water iron concentration (Johnston et al., 2014). The eventually formed FeS_x compounds could limit Fe–P formation and promote the increase of the SRP residence time in pore water. The latter was supported by the relatively strong negative correlations between SRP and S_d (τ between -0.394 in August 2020 and -0.736 in April 2021 at Marans, $p < 0.001$, Table 1). It was noticed the more heterogeneous correlations at Genouillé with highest coefficient in February and April 2020 ($\tau > 0.600$, $p < 0.001$).

The high S_d concentration in May at Marans (Fig. 2 A 20) (absence of sulphate consumption) could break the SRP mobilization initiated in April (Fig. 2 A 11), leaving a high proportion of free iron oxide able to sequester P. Although sulphate concentrations were about 30 times lower in this work than in the marine environment, it was demonstrated that sulphate consumption rates (integrated in the top 6 cm of sediment) were more than 10 times higher than dissolved iron production in August and July at Marans and Genouillé respectively (Table 2). Moreover, note that the potential for sulphate-reducing bacteria to enzymatically reduce Fe^{3+} has been highlighted in laboratory studies (Lovley et al., 1993) and in marine sediments (Wunder et al., 2021) which could be another source for Fe_d and even SRP mobilization. Fe–P dissolution in sulphate rich sediment could also occur through Fe–S complexation especially after macroalgal bloom deposition (Rozan et al., 2002).

4.3.2. Anaerobic methane oxidation and SRP mobilization

While sulphate reduction could be driven by the flux of sedimentary OM from above, it may also be derived from coupling with anaerobic methane oxidation (AOM) in freshwater wetlands (Segarra et al., 2013, 2015). The ubiquitous nature of AOM in freshwater sediment, particularly in lakes, has already been demonstrated (Martinez-Cruz et al., 2018). The linear sulphate gradient in November 2020 and April 2021 at Marans (Fig. 2 A 48, 62) and the linear sulphate gradient before total depletion in July and October 2020 at Genouillé (Fig. 2 B 27, 34, 41) could suggest a sulphate consumption driven by methane flux from below as suggested by Borowski et al. (1996). The frequent outgassing observed at both sites suggested significant methane genesis in sediment reinforced this hypothesis. At the other date, the presence of convex-up curvature profile reflected more sulphate reduction of in situ organic sedimentary matter (Borowski et al., 1996). Moreover, AOM has been demonstrated in iron rich freshwater lake sediment (Nordi et al., 2013), which could also explain in part the reduction of iron oxide, mobilization of Fe_d and thus SRP enrichment. The presence of methane could lead to a competition for Fe^{3+} and SO_4^{2-} reduction, and thus modulate SRP remobilization rates and eventual benthic effluxes.

4.4. Dissolved chemical gradient establishment and sediment homogeneity

The great heterogeneity of the chemical gradients observed in the first 6 cm of sediment contrasted with a certain vertical homogeneity of the OM and of conservative parameters such as Na_d. This homogeneity could reflect the refractory nature of the latter, contributing to the high carbon storage capacity of these environments (Kayranli et al., 2010).

The temporal variation of gradients, notably DIN, Fe_d, S_d and SRP (Fig. 2), testified the rapidity with which diagenetic processes occur in this type of system. While the evolution of P concentrations in sediments seems to be dictated by processes on a monthly scale (see 4.2), its transfer to the water column is more seasonal (Moncelon et al., 2022) and site-dependent (see 4.3). The rapidity in diagenetic processes evolution was linked to NO_3^- inputs into the system and its biological and chemical availability in the sedimentary compartment. The similar geochemical behavior of the two sites with respect to NO_3^- pulses (i. e. inhibition of SRP mobilization at SWI), despite their distinct adjacent anthropic pressure, implied the importance to integrate the entire watershed whose waters were potentially discharged into the studied canal systems. Indeed, Marans site being dominated by cereal crops (75% of drained marsh) should be more subject to local NO_3^- pollution, rather than Genouillé which was surrounded by both cattle lands and crops (study site was only surrounded by permanent grasslands). However, some reports mentioned the global catchment areas of both sites to be heavily impacted by fertilizers and in particular N which would fluctuate between 40 and 90 kg N. ha^{-1} permanently in the soil (Development and water management scheme, SAGE, of Sèvre Niortaise and Charente). This highlights the importance of diffuse pollution for NO_3^- inputs in these systems. Water management could have great impact on P transfer toward the water column Genouillé marsh showingearlier SRP efflux in the season than Maran marsh, probably due to its lower NO_3^- penetration depth (Moncelon et al., 2022). This could be due to a more diluted system in link with known freshwater injection strategies into the system (personal discussion, Atlantic Marshes Union, UNIMA).

Conversely, while the seasonal (winter and early spring) nitrate inputs seemed to be confirmed at Marans, at Genouillé several inputs seem to be recorded in surface waters, with a particular enrichment in August (Fig. 2 B 29, and Moncelon et al., 2022). The water management mentioned above could also explain such punctual inputs. However, the

short duration of these inputs and the pumping of nutrients from the water column by phytoplankton (Moncelon et al., 2022) did not seem to give nitrate time to penetrate the sediment. This raises the question of the effect of a longer nitrate residence time in surface water in summer period on the sedimentary compartment.

Moreover, the proximity of these freshwater marshes to saline environment invites to study the potential intrusion of saline water in the system. In a context of a sea level rise, soil salinization threatens coastal agricultural soils and soil microbial communities which determine consequences on fluxes of C, N and P (Mazhar et al., 2022). Variation in Na_d concentration in porewater can be a good indicator of such pore water salinization and of the temporality and nature of potential oxidant inputs for OM mineralization such as sulphates. Temporal S_d variations suggested punctual inputs of more or less marine-influenced water masses since its increase in surface seemed to be linked to those of Na_d at both sites (from July to October at Marans, May-July and January-April 2021 at Genouillé, Fig. 2). The dissolved sulphur decrease with depth despite the small vertical change in Na_d could also suggest its intrusion from the intrinsic soft water of the environment, autochthonous material or from gypsum spreading within the agricultural basin. However, S_d seemed to be rapidly involved in biotic (for OM mineralization, see below) or chemical (reduction by methane, see below) processes that could explain the mismatch between Na_d and S_d vertical profiles.

4.5. Temperature and organic matter load effects

Although the effect of nitrates on Fe, S and ultimately SRP cycles has been shown above, other seasonal factors such as sediment temperature or OM loading can synergistically impact these cycles. The fine, cohesive sediments at both sites exacerbate the effect of temperature increases and OM retention in the sediment over the seasons, favoring anaerobic respiration processes such as sulphate reduction (Al-Raei et al., 2009; Weston and Joye, 2005). This coincided with higher sulphate and even iron oxide reduction rates in August and July at Marans and Genouillé respectively (Table 2), when OM levels in sediments are high (Fig. 1).

In addition, factors such as bioturbation or the presence of macrophytes, enhanced by spring/summer season, can promote the reduction of iron oxides by regenerating oxidation processes or by promoting chemical exchanges (Kostka et al., 2002a, 2002b). Conversely, it has been shown the iron-reducing bacteria inhibition in summer period by the increase in sulphate-reduction processes which, following sulphide production, promote the abiotic reduction of bioavailable Fe^{3+} (Koretsky et al., 2003). These two late processes promote the release of SRP in porewater (cf. 4.1.2).

Concerning the N cycle, the low superficial sediment NO_3^- concentrations in summer and late summer at both sites (Fig. 2) were probably linked to biological N fixation in the water column at that time (Moncelon et al., 2021, 2022), limiting its penetration into the sediment. It could, however, be regenerated via sedimentary sources of ammonium. Indeed, the strong $\sum NH_3$ gradient in pore waters in winter could contribute to the overlying water input and the NO_3^- regeneration via nitrification process. This $\sum NH_3$ did not appear to be affected by biogeochemical processes at the studied sediment depths, further supporting the idea of NO_3^-/NO_2^- regeneration in the water column. These deep sources of $\sum NH_3$ in winter could suppose the mineralization (below the depths studied) of intense inputs of older OM.

5. Conclusion

The yearly geochemical monitoring of two drained and P-limited freshwater marshes explored the main processes responsible for the SRP mobilization in the sediment. The classic diagenetic succession seemed to be controlled by the high punctual inputs of nitrate, according to the water management in the drained marsh. These inputs especially seemed to promote the establishment and stability of an iron curtain ((oxy)hydroxides-enriched layer that retained P through adsorption). The phosphate recycling dynamics seemed more complex than controlled solely by the presence of nitrate, and the importance of the sulphur cycle has been highlighted in terms of controlling the iron curtain thickness and efficiency. These results encourage the real quantification of processes responsible of SRP mobilization in the sediment. This would improve action points if eutrophication event occurred, especially in P limited freshwater system. More than propose a detailed description of annual functioning of sediment compartment, this work highlighted the potential capacity of drained marsh soils to protect the aquatic environment against pollution such as over-fertilization, by trapping (P) and mitigating crucial nutrients (N) for the overall functioning of these environments. Such knowledges are essential for a better water management in an anthropized land-sea continuum since the risks of eutrophication in coastal areas depend on algal bloom trigger events, such as nutrient mobilization sources.

CRediT authorship contribution statement

Raphaël Moncelon: Writing – review & editing, Writing – original draft, Visualization, Validation, Methodology, Investigation, Formal analysis, Data curation, Conceptualization. **Christine Dupuy:** Writing – review & editing, Validation, Supervision, Methodology, Investigation, Funding acquisition, Formal analysis, Conceptualization. **Philippe Pineau:** Validation, Investigation, Formal analysis. **Claire Emery:** Validation, Investigation, Formal analysis. **Eric Bénéteau:** Validation, Formal analysis. **Olivier Philippine:** Validation, Conceptualization. **François-Xavier Robin:** Validation, Conceptualization. **Edouard Metzger:** Writing – review & editing, Validation, Supervision, Methodology, Investigation, Formal analysis, Conceptualization.

Declaration of competing interest

The authors declare that they have no known competing financial interests or personal relationships that could have appeared to influence the work reported in this paper.

Acknowledgments

This study was supported by the « Ministère de l'Enseignement Supérieur et de la Recherche », the water agencies Loire-Bretagne and Adour-Garonne, the General Council of Charente-Maritime, the European Union. This research was supported by a PhD grant from the La Rochelle conurbation (CDA). We acknowledge the LIENSs AutoAnalyzer platform for nutrient analyses and the "Radioécology lab" for production measurements and the LPG geochemical analytic platform for ICPAES analyses. Thanks, are extended to the UNIMA (Union des Marais de Charente-Maritime), FMA and stakeholders for their expertise on the Charente-Maritime marshes. The authors want to thank the anonymous reviewers for their valuable help at improving this manuscript.

Appendix A. Supplementary data

Supplementary data to this article can be found online at https://doi.org/10.1016/j.apgeochem.2024.106200.

Data availability

Data will be made available on request.

References

Aller, R.C., 2004. Conceptual models of early diagenetic processes: the muddy seafloor as an unsteady, batch reactor. J. Mar. Res. 62, 815–835.

Al-Raei, A.M., Bosselmann, K., Böttcher, M.E., Hespenheide, B., Tauber, F., 2009. Seasonal dynamics of microbial sulfate reduction in temperate intertidal surface sediments: controls by temperature and organic matter. Ocean Dyn 59, 351–370.

Anschutz, P., Zhong, S., Sundby, B., Mucci, A., Gobeil, C., 1998. Burial efficiency of phosphorus and the geochemistry of iron in continental margin sediment. Limnol. Oceanogr. 43, 53–64.
Bethke, C.M., Sanford, R.A., Kirk, M.F., Jin, Q., Flynn, T.M., 2011. The thermodynamic ladder in geomicrobiology. Am. J. Sci. 311, 183–210.
Borowski, W.S., Paull, C.K., Ussler, W., 1996. Marine pore-water sulfate profiles indicate in situ methane flux from underlying gas hydrate. Geology 24, 655–658.
Cañedo-Argüelles, M., Kefford, B.J., Piscart, C., Prat, N., Schäfer, R.B., Schulz, C.J., 2013. Salinisation of rivers: an urgent ecological issue. Environ. Pollut. 173, 157–167.
Chen, F., Xia, Q., Ju, L.K., 2005. Competition between oxygen and nitrate respirations in continuous culture of pseudomonas aeruginosa performing aerobic denitrification. Biotechnol. Bioeng. 93, 1069–1078.
Christensen, K.K., Andersen, F.E., Jensen, H.S., 1997. Comparison of iron, manganese, and phosphorus retention in freshwater littoral sediment with growth of Littorella uniflora and benthic microalgae. Biogeochemistry 38, 149–171.
Conley, D.J., Paerl, H.W., Howarth, R.W., Boesch, D.F., Seitzinger, S.P., Havens, K.E., Lancelot, C., Likens, G.E., 2009. Controlling eutrophication: phosphorus and nitrogen. Science 323, 1014–1015.
Feng, Z., Fan, C., Huang, W., Ding, S., 2014. Microorganisms and typical organic matter responsible for lacustrine "black bloom." Sci. Total Environ 470/471, 1–8.
Froelich, P.N., Klinkhammer, G.P., Bender, M.L., Luedtke, N.A., Heath, G.R., Cullen, D., Dauphin, P., Hammond, D., Hartman, B., Maynard, V., 1979. Early oxidation of organic matter in pelagic sediments of the eastern equatorial Atlantic: suboxic diagenesis. Geochem. Cosmochim. Acta 43, 1075–1090.
Gächter, R., Müller, B., 2003. Why the phosphorus retention of lakes does not necessarily depend on the oxygen supply to their sediment surface. Limnol. Oceanogr. 48, 929–933.
Glock, N., Roy, A.S., Romero, D., Wein, T., Weissenbach, J., Revsbech, N.P., Høgslund, S., Clemens, D., Sommer, S., Dagan, T., 2019. Metabolic preference of nitrate over oxygen as an electron acceptor in foraminifera from the Peruvian oxygen minimum zone. Proc. Natl. Acad. Sci. U.S.A. 116, 2860–2865.
Grüneberg, B., Dadi, T., Lindim, C., Fischer, H., 2014. Effects of nitrogen and phosphorus load reduction on benthic phosphorus release in a riverine lake. Biogeochemistry 123, 185–202.
Hauck, S., Benz, M., Brune, A., Schink, B., 2001. Ferrous iron oxidation by denitrifying bacteria in profundal sediments of a deep lake (Lake Constance). FEMS Microbiol. Ecol. 37, 127–134.
Herbert, E.R., Boon, P., Burgin, A.J., Neubauer, S.C., Franklin, R.B., Ardon, M., Hopfensperger, K.N., Lamers, L.P.M., Gell, P., Langley, J.A., 2015. A global perspective on wetland salinization: ecological consequences of a growing threat to freshwater wetlands. Ecosphere 6, 1–43.
Herzsprung, P., Schultze, M., Hupfer, M., Boehrer, B., Tümpling, W.v., Duffek, A., Duffek, A., Van der Veen, A., Friese, K., 2010. Flood effects on phosphorus immobilisation in a river water filled pit lake-case study lake Goitsche (Germany). Limnologica 40, 182–190.
Hogan, J.F., Phillips, F.M., Mills, S.K., Hendrickx, J.M.H., Ruiz, J., Chesley, J.T., Asmerom, Y., 2007. Geologic origins of salinization in a semi-arid river: the role of sedimentary basin brines. Geology 35, 1063–1066.
Howarth, W., 2011. Diffuse water pollution and diffuse environmental laws: tackling diffuse water pollution in england, report by the comptroller and auditor general. J. Environ. Law 23, 129–141.
Jin, P.K., Yang, Z.R., Li, R., Li, Y., Zhou, L.H., 2017. Characteristics of. Denitrification Inhibiting Sulfate Reducing Process 38, 1982–1990. https://doi.org/10.13227/j.hjkx.201611097.
Johnston, S.G., Burton, E.D., Aaso, T., Tuckerman, G., 2014. Sulfur, iron and carbon cycling following hydrological restoration of acidic freshwater wetlands. Chem. Geol. 371, 9–26.
Kayranli, B., Scholz, M., Mustafa, A., Hedmark, Å., 2010. Carbon storage and fluxes within freshwater wetlands: a critical review. Wetlands 30, 111–124.
Köhler, J., Hilt, S., Adrian, R., Nicklisch, A., Kozerski, H.P., Walz, N., 2005. Long-term response of a shallow, moderately flushed lake to reduced external phosphorus and nitrogen loading. Freshw. Biol. 50, 1639–1650.
Koretsky, C.M., Moore, C.M., Lowe, K.L., Meile, C., Dichristina, T.J., Van Cappellen, P., 2003. Seasonal oscillation of microbial iron and sulfate reduction in saltmarsh sediments (Sapelo Island, GA, USA). Biogeochemistry 64, 179–203.
Kostka, J.E., Gribsholt, B., Petrie, E., Dalton, D., Skelton, H., Kristensen, E., 2002a. The rates and pathways of carbon oxidation in bioturbated saltmarsh sediments. Limnol. Oceanogr 47, 230–240.
Kostka, J.E., Luther, G.W., 1994. Partitioning and speciation of solid phase iron in saltmarsh sediments. Geochem. Cosmochim. Acta 58, 1701–1710.
Kostka, J.E., Roychoudhury, A., Van Cappellen, P., 2002b. Rates and controls of anaerobic microbial respiration across spatial and temporal gradients in saltmarsh sediments. Biogeochemistry 60, 49–76.
Lamers, L.P.M., Sarah-J, F., Samborska, E.M., Van Dulken, I.A.R., Van Hengstum, G., Roelofs, J.G.M., 2002. Factors controlling the extent of eutrophication and toxicity in sulfate-polluted freshwater wetlands. Limnol. Oceanogr. 47, 585–593.
Le Moal, M., Gascuel-Odoux, C., Ménesguen, A., Souchon, Y., Étrillard, C., Levain, A., Moatar, F., Pannard, A., Souchu, P., Lefebvre, A., Pinay, G., 2019. Eutrophication: a new wine in an old bottle? Sci. Total Environ. 651, 1–11.
Lin, C.Y., Bradbury, H.J., Antler, G., Burdige, D.J., Bennett, T.D., Li, S., Turchyn, A.V., 2022. Sediment mineralogy influences the rate of microbial sulfate reduction in marine sediments. Earth Planet Sci. Lett. 598, 117841.
Louis, J., Jeanneau, L., Andrieux-Loyer, F., Gruau, G., Caradec, F., Lebris, L., Chorin, M., Jardé, E., Rabiller, E., Petton, E., Bouger, G., Petitjean, P., Laverman, M., M, A., 2021. Are benthic nutrient fluxes from intertidal mudflats driven by surface sediment characteristics? Compt. Rendus Geosci. 353, 173–191.
Lovley, D.R., Roden, E.E., Phillips, E.J.P., Woodward, J.C., 1993. Enzymatic iron and uranium reduction by sulfate-reducing bacteria. Mar. Geol. 113, 41–53.
Ma, W., Zhu, M., Yang, G., Li, T., 2017. In situ, high-resolution DGT measurements of dissolved sul fi de, iron and phosphorus in sediments of the East China Sea : Insights into phosphorus mobilization and microbial iron reduction. Mar. Pollut. Bull. 124, 400–410.
Marsden, M.W., 1989. Lake restoration by reducing external phosphorus loading: the influence of sediment phosphorus release. Freshw. Biol. 21, 139–162.
Martinez-Cruz, K., Sepulveda-Jauregui, A., Casper, P., Anthony, K.W., Smemo, K.A., Thalasso, F., 2018. Ubiquitous and significant anaerobic oxidation of methane in freshwater lake sediments. Water Res. 144, 332–340.
Melton, E.D., Schmidt, C., Kappler, A., 2012. Microbial iron(II) oxidation in littoral freshwater lake sediment: the potential for competition between phototrophic vs. nitrate-reducing iron(II)-oxidizers. Front. Microbiol. 3, 1–12.
Metzger, E., Simonucci, C., Viollier, E., Sarazin, G., Prévot, F., Jézéquel, D., 2007. Benthic response to shellfish farming in Thau lagoon: pore water signature. Estuar. Coast Shelf Sci. 72, 406–419.
Millero, F.J., Sotolongo, S., Izaguirre, M., 1987. Oxidation kinetics of Fe (II) in sea water. Geochem. Cosmochim. Acta 51, 793–801.
Moncelon, R., Gouazé, M., Pineau, P., Bénéteau, E., Bréret, M., Philippine, O., Robin, F. X., Dupuy, C., Metzger, E., 2021. Coupling between sediment biogeochemistry and phytoplankton development in a temperate freshwater marsh (Charente-Maritime, France): evidence of temporal pattern. Water Res. 189, 116567.
Moncelon, R., Metzger, E., Pineau, P., Emery, C., Bénéteau, E., de Lignières, C., Philippine, O., Robin, F.X., Dupuy, C., 2022. Drivers for primary producers' dynamics: new insights on annual benthos pelagos monitoring in anthropized freshwater marshes (Charente-Maritime, France). Water Res. 221, 118718.
Neupane, G., Donahoe, R.J., Arai, Y., 2014. Kinetics of competitive adsorption/desorption of arsenate and phosphate at the ferrihydrite-water interface. Chem. Geol. 368, 31–38.
Ni, Z., Wang, S., Cai, J., Li, H., Jenkins, A., Maberly, S.C., May, L., 2019. The potential role of sediment organic phosphorus in algal growth in a low nutrient lake. Environ. Pollut 255, 113235.
Nordi, K.Á., Thamdrup, B., Schubert, C.J., 2013. Anaerobic oxidation of methane in an iron-rich Danish freshwater lake sediment. Limnol. Oceanogr. 58, 546–554.
Nürnberg, G.K., Tarvainen, M., Ventelä, A.M., Sarvala, J., 2012. Internal phosphorus load estimation during biomanipulation in a large polymictic and mesotrophic lake. Inl. Waters 2, 147–162.
Ockenden, M.C., Deasy, C., Quinton, J.N., Surridge, B., Stoate, C., 2014. Keeping agricultural soil out of rivers: evidence of sediment and nutrient accumulation within field wetlands in the UK. J. Environ. Manag. 135, 54–62.
Oshiki, M., Ishii, S., Yoshida, K., Fujii, N., Ishiguro, M., Satoh, H., Okabe, S., 2013. Nitrate-dependent ferrous iron oxidation by anaerobic ammonium oxidation (anammox) bacteria. Appl. Environ. Microbiol. 79, 4087–4093.
Perkins, R.G., Underwood, G.J.C., 2001. The potential for phosphorus release across the sediment-water interface in an eutrophic reservoir dosed with ferric sulphate. Water Res. 35, 1399–1406.
Petzoldt, T., Uhlmann, D., 2006. Nitrogen emissions into freshwater ecosystems: is there a need for nitrate elimination in all wastewater treatment plants? Acta Hydrochim. Hydrobiol. (Sofia) 34, 305–324.
Rockström, J., Steffen, W., Noone, K., Persson, A., Chapin III, F.S., Lambin, E.F., Lenton, T.M., Scheffer, M., Folke, C., Schellnhuber, H.J., Nykvist, B., de Wit, C.A., Hughes, T., van der Leeuw, S., Rodhe, H., Sörlin, S., Snyder, P.K., Costanza, R., Svedin, U., Falkenmark, M., Karlberg, L., Corell, R.W., Fabry, V.J., Hansen, J., Walker, B., Liverman, D., Richardson, K., Crutzen, P., Foley, J.A., 2009. A safe operating space for humanity. Nature 461, 472–475.
Rozan, T.F., Taillefert, M., Trouwborst, R.E., Glazer, B.T., Ma, S., Herszage, J., Valdes, L. M., Price, K.S., Luther, G.W., 2002. Iron-sulfur-phosphorus cycling in the sediments of a shallow coastal bay: implications for sediment nutrient release and benthic macroalgal blooms. Limnol. Oceanogr. 47, 1346–1354.
Sarazin, G., Michard, G., Prevot, F., 1999. A rapid and accurate spectroscopic method for alkalinity measurements in sea water samples. Water Res. 33, 290–294.
Schindler, D.W., 1977. Evolution of phosphorus limitation in lakes. Science 195, 260–262.
Schindler, D.W., Carpenter, S.R., Chapra, S.C., Hecky, R.E., Orihel, D.M., 2016. Reducing phosphorus to curb lake eutrophication is a success. Environ. Sci. Technol. 50, 8923–8929.
Segarra, K.E.A., Comerford, C., Slaughter, J., Joye, S.B., 2013. Impact of electron acceptor availability on the anaerobic oxidation of methane in coastal freshwater and brackish wetland sediments. Geochem. Cosmochim. Acta 115, 15–30.
Segarra, K.E.A., Schubotz, F., Samarkin, V., Yoshinaga, M.Y., Hinrichs, K.U., Joye, S.B., 2015. High rates of anaerobic methane oxidation in freshwater wetlands reduce potential atmospheric methane emissions. Nat. Commun. 6, 2–9.
Sinha, E., Michalak, M., Alaji, V., 2017. Eutrophication will increase over the 21 st century due to precipitation changes. Science 357, 405–408.
Smith, V.H., 2003. Eutrophication of freshwater and coastal marine ecosystems a global problem. Environ. Sci. Pollut. Res. 10, 126–139.
Søndergaard, M., Lauridsen, T.L., Johansson, L.S., Jeppesen, E., 2017. Nitrogen or phosphorus limitation in lakes and its impact on phytoplankton biomass and submerged macrophyte cover. Hydrobiologia 795, 35–48.
Stotzky, G., Rem, L.T., 1966. Influence of clay minerals on microorganisms. I. Montmorillonite and kaolinite on bacteria. Can. J. Microbiol. 12, 547–563.
Thamdrup, B., Canfield, D.E., 2000. Benthic respiration in aquatic sediments. Methods ecosyst. Sci 86–103.

Thibault de Chanvalon, A., Metzger, E., Mouret, A., Knoery, J., Geslin, E., Meysman, F.J. R., 2017. Two dimensional mapping of iron release in marine sediments at submillimetre scale. Mar. Chem. 191, 34–49.
Tortajada, S., David, V., Brahmia, A., Dupuy, C., Laniesse, T., Parinet, B., Pouget, F., Rousseau, F., Simon-Bouhet, B., Robin, F.X., 2011. Variability of fresh- and salt-water marshes characteristics on the west coast of France: a spatio-temporal assessment. Water Res. 45, 4152–4168.
Ulén, B., Bechmann, M., Fölster, J., Jarvie, H.P., Tunney, H., 2007. Agriculture as a phosphorus source for eutrophication in the north-west European countries, Norway, Sweden, United Kingdom and Ireland: a review. Soil Use Manag. 23, 5–15.
van Dael, T., De Cooman, T., Verbeeck, M., Smolders, E., 2020. Sediment respiration contributes to phosphate release in lowland surface waters. Water Res. 168, 115168.
Vile, M.A., Bridgham, S.D., Wieder, R.K., 2003. Response of anaerobic carbon mineralization rates to sulfate amendments in a boreal peatland. Ecol. Appl. 13, 720–734.
Vymazal, J., 2011. Enhancing ecosystem services on the landscape with created, constructed and restored wetlands. Ecol. Eng. 37, 1–5.
Wauer, G., Gonsiorczyk, T., Casper, P., Koschel, R., 2005. P-immobilisation and phosphatase activities in lake sediment following treatment with nitrate and iron. Limnologica 35, 102–108.
Weston, N.B., Joye, S.B., 2005. Temperarure driven decoupling a key phases of organic matter degradation in marine sediments. Proc. Natl. Acad. Sci. USA 102, 17036–17040.
Wood, F.L., Heathwaite, A.L., Haygarth, P.M., 2005. Evaluating diffuse and point phosphorus contributions to river transfers at different scales in the Taw catchment, Devon, UK. J. Hydrol 304, 118–138.
Wunder, L.C., Aromokeye, D.A., Yin, X., Richter-Heitmann, T., Willis-Poratti, G., Schnakenberg, A., Otersen, C., Dohrmann, I., Römer, M., Bohrmann, G., Kasten, S., Friedrich, M.W., 2021. Iron and sulfate reduction structure microbial communities in (sub-)Antarctic sediments. ISME J. 15, 3587–3604.
Zhu, B., Friedrich, S., Wang, Z., Táncsics, A., Lueders, T., 2020. Availability of nitrite and nitrate as electron acceptors modulates anaerobic toluene-degrading communities in aquifer sediments. Front. Microbiol. 11, 1867.